A Zero-Voltage-Switched PWM Boost Converter with an Energy Feedforward Auxiliary Circuit

Gerry Moschopoulos, *Member, IEEE*, Praveen K. Jain, *Senior Member, IEEE*, Yan-Fei Liu, *Senior Member, IEEE*, and Géza Joós, *Senior Member, IEEE*

***Abstract*— A zero-voltage-switched (ZVS) pulsewidth-modulated (PWM) boost converter with an energy feedforward auxiliary circuit is proposed in this paper. The auxiliary circuit, which is a resonant circuit consisting of a switch and passive components, ensures that the converter's main switch and boost diode operate with soft switching. This converter can function with PWM control because the auxiliary resonant circuit operates for a small fraction of the switching cycle. Since the auxiliary circuit is a resonant circuit, the auxiliary switch itself has both a soft turn on and turn off, resulting in reduced switching losses and electromagnetic interference (EMI). This is unlike other proposed ZVS boost converters with auxiliary circuits where the auxiliary switch has a hard turn off. Peak switch stresses are only slightly higher than those found in a conventional PWM boost converter because part of the energy that would otherwise circulate in the auxiliary circuit and drastically increase peak switch stresses is fed to the load. In this paper, the operation of the converter is explained and analyzed, design guidelines are given, and experimental results obtained from a prototype are presented. The proposed converter is found to be about 2%–3% more efficient than the conventional PWM boost converter.**

***Index Terms*—Power factor correction, PWM, soft switching, zero-voltage switching.**

I. Introduction

The pulsewidth-modulated (PWM) boost converter is widely used as a dc–dc converter and as a power-factor-correction (PFC) preregulator for power supplies. The boost converter operated in the continuous conduction mode is in fact the most popular topology used in industry today for PFC. This converter, however, has several problems due to the reverse recovery of the boost diode and the switching losses of the boost switch. During the diode's reverse recovery time, which occurs whenever the switch is turned on, a high and sharp negative spike appears in the diode current because there is a temporary shootthrough of the output capacitor to ground (as the full output voltage is placed across the switch). This spike results in increased electromagnetic interference (EMI) and losses in the diode. The switching losses of the boost switch, which is typically a MOSFET, consist of turn-off and turn-on losses. The turn-off losses are caused by the switch having simultaneous nonzero current and voltage while it is turning off, and the turn-on losses are caused by the energy stored in the drain–source capacitance that is dissipated in the switch during turn on. These losses lead to a significant decrease in converter efficiency.

In recent years, several zero-voltage-transition (ZVT) boost converters [1]–[7] have been proposed to try to overcome the above problems. All these converters have an auxiliary circuit that is added to the main boost converter and used to ensure that the boost diode has a soft turn off and the boost switch is turned on with zero-voltage switching (ZVS). The auxiliary circuit consists of a switch and passive components and is in operation only when current is transferred from the boost diode to the main switch. Except for this particular time interval, ZVT converters operate exactly like PWM converters.

The ZVT boost converters that have been proposed in the literature, however, have at least one of the following drawbacks.

1) Soft switching of the main switch is achieved by using an auxiliary switch that does not have a lossless turn off. Additional turn-off losses are caused by the presence of a dissipative snubber that must be used to minimize oscillations caused by the interaction of an auxiliary circuit inductor with the output capacitance of the auxiliary switch (i.e., [2] and [4]).
2) A substantial amount of EMI is created by the auxiliary circuit ([1], [2], and [8]). In fact, this EMI is almost equivalent to that produced by the boost diode reverse recovery current in a conventional PWM converter. This is especially true in cases where the auxiliary switch turn-off losses are minimized by turning off the switch very quickly to reduce the time when there is both voltage across and current flowing through the switch.
3) The switches in converters with a resonant auxiliary circuit have high-voltage stresses and/or current stresses. In some proposed converters, these stresses can exceed twice the stresses found in standard PWM boost converters [3], [6].
4) The converter cannot be used in PFC applications, but only as a dc–dc converter. For example, a boost converter is proposed in [7] that feeds auxiliary circuit energy to the input. This technique can only work if the input is fixed and nonvarying, which is not the case when the source is ac.
5) The auxiliary switch requires a floating gate drive, which increases the complexity of the converter.

Manuscript received May 5, 1997; revised December 14, 1998. Recommended by Associate Editor, K. Smedley.

G. Moschopoulos, P. K. Jain, and G. Joós are with the P. D. Ziogas Laboratory, Department of Electrical and Computer Engineering, Concordia University, Montréal, P.Q., H3G 1M8, Canada.

Y.-F. Liu is with Astec, Station C, Ottawa, Ont., K1Y 4H7, Canada.

Publisher Item Identifier S 0885-8993(99)05557-X.

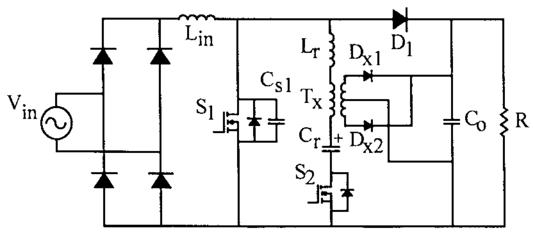

Fig. 1. The proposed ZVT PWM boost converter.

The ZVT boost converter proposed in this paper (Fig. 1) does not have the above limitations. The key feature of this converter is that a nearly lossless auxiliary switch turn off is achieved with a soft instead of a hard turn off, which limits EMI. Moreover, the energy feedforward diodes D_{x1} and D_{x2} have less reverse recovery current than that found in similar diodes in other ZVT topologies. This is because D_{x1} and D_{x2} conduct only a fraction of the auxiliary circuit current since the auxiliary circuit transformer steps it down. Although the operation of the auxiliary circuit does cause the main switch to operate with a resonant current peak, this peak is lower than that found in other proposed converters. In this paper, the operation of the converter is explained and analyzed, and design guidelines are given. The feasibility of the proposed converter is shown with experimental results obtained from a 500-W 50-kHz prototype operating with PFC.

II. Circuit Description and Principles of Operation

The proposed converter consists of a diode bridge rectifier, main switch S_1 and auxiliary switch S_2, boost diode D_1, energy recovery diodes D_{x1} and D_{x2}, inductors L_{in} and L_r, capacitors C_o, C_{s1}, and C_r, and transformer T_x. Resistor R represents the load. Components L_{in}, S_1, D_1, and C_o make up a standard boost converter. Unity input power factor is achieved by switching S_1 so that the current through L_{in} is shaped to be sinusoidal and in phase with the input voltage. Capacitor C_o is used to reduce the harmonic ripple found on the output voltage. Capacitor C_{s1} is placed across S_1 to reduce switching losses and EMI during turn off. The remaining converter components comprise the auxiliary circuit.

The main boost switch in Fig. 1 is turned on with ZVS by activating the auxiliary circuit and discharging C_{s1} just before turn on is to occur. The auxiliary switch has a zero-current-switched (ZCS) turn on and a ZVS turn off because of the series LC circuit in the auxiliary circuit: The ZCS turn on is due to inductor L_r, which slows down the rate of current rise through S_2, and the ZVS turn off is caused by the resonant circuit injecting current through the diode across S_2. Since the body diode found in presently available devices has a slow reverse recovery, it is therefore recommended that the body diode of S_2 be blocked by placing a diode in series with it and a fast recovery diode in parallel with the series diode–switch combination.

The auxiliary circuit losses and component stresses can be decreased by reducing the amount of energy circulating in the auxiliary circuit while it is in operation. The purpose of transformer T_x and diodes D_{x1} and D_{x2} is to provide a path

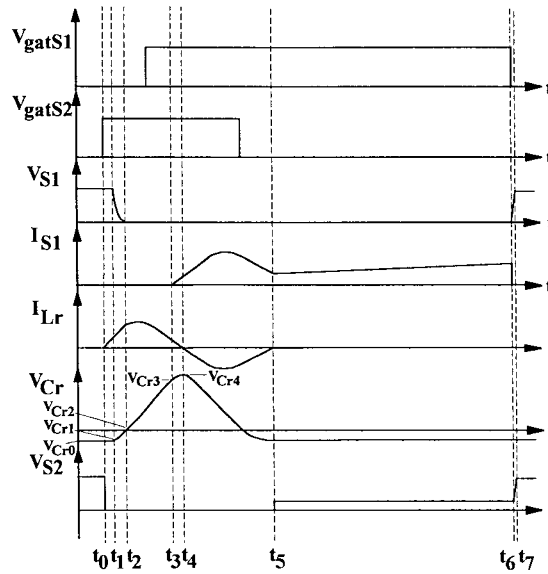

Fig. 2. Gating signal and circuit waveforms.

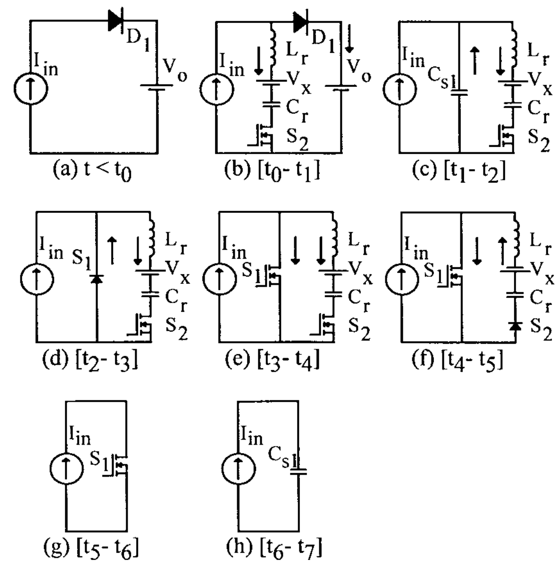

Fig. 3. Intervals of converter operation over a complete switching cycle.

for part of this energy to be fed to the load. Such a path is always present during auxiliary circuit operation because current can flow through either D_{x1} and D_{x2}. When auxiliary circuit current is flowing in the positive direction, a voltage is impressed across the primary of T_x, and the secondary voltage makes diode D_{x1} conduct. Likewise, diode D_{x2} conducts when current in the auxiliary circuit is flowing in the negative direction. In both cases, the primary voltage is clamped to a magnitude of V_o/N_x, where N_x is the turns ratio of T_x.

The proposed converter has eight operating intervals for one switching cycle. Gating signals and circuit waveforms are shown in Fig. 2, and the equivalent circuit for each interval is shown in Fig. 3. The operating intervals are as follows.

1) Interval 0 $[t < t_0]$*:* The main switch S_1 and the auxiliary switch S_2 are both off, and current is flowing to the load through diode D_1. The auxiliary circuit capacitor C_r is charged to a voltage, V_{Cr0}, which is negative.

2) Interval 1 $[t_0 - t_1]$: The auxiliary switch S_2 is turned on with resonant inductor L_r limiting the rate of current rise. Current is diverted from diode D_1 and the current flowing through the auxiliary circuit rises. At the end of this interval, the current flowing through the auxiliary circuit is equal to the input current, and the voltage across the resonant capacitor is V_{Cr1}.

3) Interval 2 $[t_1 - t_2]$: Current stops flowing through diode D_1 at $t = t_1$ and the current flowing through the auxiliary circuit I_{Lr} is greater than the input current. As I_{Lr} continues to rise, the current that exceeds the input current discharges the capacitor across S_1, C_{s1}. This interval ends when C_{s1} has been fully discharged. When this happens, the current flowing through the auxiliary circuit is equal to I_{Lr2}, and the voltage across the resonant capacitor is V_{Cr2}.

4) Interval 3 $[t_2 - t_3]$: After $t = t_2$, the antiparallel diode of S_1 conducts, keeping the voltage across the switch at zero and allowing the switch to be turned on with ZVS. The current flowing through the auxiliary circuit at the end of the interval is the same as the input current.

5) Interval 4 $[t_3 - t_4]$: Current begins to flow through S_1 after $t = t_3$, and the current flowing through the auxiliary circuit is still positive, but less than the input current. At the end of this interval, current I_{Lr} is zero and the voltage across C_r is $V_{Cr} = V_{Cr4}$.

6) Interval 5 $[t_4 - t_5]$: Current is flowing through the main switch S_1. This current is the sum of the input current and the current flowing through the auxiliary circuit, through the antiparallel diode across S_2. The auxiliary switch S_2 is turned off with ZVS. Under steady-state conditions, the value of V_{Cr} after this interval is the same as it was before the auxiliary circuit was activated: $V_{Cr} = V_{Cr1}$.

7) Interval 6 $[t_5 - t_6]$: The converter operates exactly like a standard PWM boost converter during this interval because the auxiliary circuit is not in operation.

8) Interval 7 $[t_6 - t_7]$: At the start of this interval, S_1 is turned off and capacitor C_{s1} begins to charge. Since C_{s1} limits the rate of voltage rise, there is little voltage across the switch when it is turned off. C_{s1} is charged until the voltage across it is equal to the output voltage. Current then starts flowing through diode D_1 and continues to do until the auxiliary circuit is reactivated.

III. CIRCUIT ANALYSIS

The equations that characterize each interval of auxiliary circuit operation described in Section II are presented in this section. Only the key auxiliary circuit interval equations are presented because the proposed converter behaves like a conventional PWM boost converter during most of the switching cycle except when the auxiliary circuit is operating. The equations have been derived using the following assumptions.

1) The input inductor L_{in} is large enough to be considered as a constant dc current source I_{in} during the time that current is flowing through the auxiliary circuit.
2) The output filter capacitor C_o is large enough to be considered as a voltage source V_o during the switching cycle.
3) The auxiliary switch S_2 has a resistance of R_r when it is turned on.
4) All inductors, capacitors, and the main switch S_1 have a negligible resistance.
5) The voltage across transformer T_x is clamped to a voltage $V_x = V_o/N_x$ by one of the transformer secondary diodes when current is flowing in the auxiliary circuit. The polarity of V_x depends on the polarity of the auxiliary circuit current.

It should be noted that V_{CrX} and I_{LrX} are the values of V_{Cr} and I_{Lr} after Interval X. The equations above have been verified in [9] with simulated and experimental results.

The equations that characterize Interval 1 are

$$I_{L_r} = \frac{V_o - V_x - V_{Cr0}}{\omega_r L_r} e^{-\xi t} \sin \omega_r t \tag{1}$$

$$V_{Cr} = V_o - V_x - \frac{\omega_o}{\omega_r} (V_o - V_x - V_{Cr0}) e^{-\xi t} \cdot \cos(\omega_r t - \psi) \tag{2}$$

where

$$\xi = \frac{R_r}{2L_r} \tag{3}$$

$$\omega_o = \frac{1}{\sqrt{L_r C_r}} \tag{4}$$

$$\omega_r = \sqrt{\omega_o^2 - \xi^2} \tag{5}$$

$$\psi = \tan^{-1} \frac{\xi}{\omega_r}. \tag{6}$$

The equations for Interval 2 are

$$I_{L_r} = e^{-\xi t}(A \cos \omega_r' t + B \sin \omega_r' t) + I_{\text{in}} \frac{C_p}{C_{s1}} \tag{7}$$

$$V_{C_{s1}} = e^{-\xi t}\left(\frac{E}{C_{s1}} \cos \omega_r' t + \frac{F}{C_{s1}} \sin \omega_r' t\right) + I_{\text{in}} \frac{C_{s1} - C_p}{C_{s1}^2} t + V_o - \frac{E}{C_{s1}} \tag{8}$$

$$V_{Cr} = -e^{-\xi t}\left(\frac{E}{C_r} \cos \omega_r' t + \frac{F}{C_r} \sin \omega_r' t\right) + I_{\text{in}} \frac{C_p}{C_r C_{s1}} t + V_{Cr1} + \frac{E}{C_r} \tag{9}$$

where

$$C_p = \frac{C_r C_{s1}}{C_r + C_{s1}} \tag{10}$$

$$A = I_{\text{in}} \frac{C_p}{C_r} \tag{11}$$

$$B = \frac{V_o - V_x - V_{Cr1} - I_{\text{in}} R_r + L_r \xi A}{\omega_r' L_r} \tag{12}$$

$$E = \frac{\xi A + B \omega_r'}{\omega_o'^2} \tag{13}$$

$$F = \frac{\xi B - A \omega_r'}{\omega_o'^2}. \tag{14}$$

The values for variables ω_o' and ω_r' can be found by substituting C_p for C_r in (4) and (5).

The equations for Intervals 3 and 4 are

$$I_{Lr} = e^{-\xi t}\left(I_{Lr2}\cos\omega_r t - \frac{G + L_r \xi I_{Lr2}}{\omega_r L_r}\sin\omega_r t\right) \quad (15)$$

$$V_{Cr} = e^{-\xi t}\left(G\cos\omega_r t + \frac{\xi C_r G + I_{Lr2}}{\omega_r C_r}\sin\omega_r t\right) - V_x \quad (16)$$

where

$$G = V_{Cr2} + V_x. \quad (17)$$

The equations for Interval 5 are

$$I_{Lr} = -\frac{V_{Cr4} - V_x}{\omega_o L_r}\sin\omega_o t \quad (18)$$

$$V_{Cr} = (V_{Cr4} - V_x)\cos\omega_o t + V_x. \quad (19)$$

The auxiliary circuit is in state state when V_{Cr} after Interval 5 is equal to V_{Cr0}.

IV. Characteristic Curves

This section presents characteristic curves for auxiliary switch voltage, auxiliary switch peak current, and main switch peak current (Fig. 4). These curves, which have been generated by computer using the equations presented in the previous section, are used in the design example presented in Section VI. Although the equations were derived with a dc input source, they can also be used to determine worst case operating conditions for the converter operating with an ac input source, which is the case when it is used PFC applications. An ac input source can be considered to be dc during a very short switching cycle.

As an example of how the equations derived in Section III can be used, Fig. 5 shows a simple flowchart of a computer program that determines whether the auxiliary circuit is functioning under steady-state conditions. This is done by determining whether the voltage across capacitor C_r, V_{Cr}, after the auxiliary circuit has gone through a cycle, is equal to its initial value before the auxiliary circuit was activated. Once it has been determined that the auxiliary circuit is in steady state, the desired value of a desired voltage or current (i.e., main switch peak current) can be determined for a specific operating point. When this is done, the whole process can be repeated for several operating points until a curve is generated.

Since the auxiliary circuit is activated just before the main switch is turned on, the operation of the circuit is dependent on the input current value at that instant, and the output voltage V_o. The curves have thus been generated with respect to the ratio

$$Z_{rb} = \frac{V_o}{I_{\text{in}}}. \quad (20)$$

The parameter on the vertical axis of each graph has been plotted with respect to the characteristic resonant impedance of auxiliary circuit components L_r and C_r

$$Z_r = \sqrt{\frac{L_r}{C_r}} \quad (21)$$

for various values of $K = C_r/C_{s1}$. The curves in Fig. 4 have been generated with $Z_{rb} = 60$ and auxiliary circuit transformer turns ratio $N_x = 8$ in accordance with the design example presented in Section VI. The vertical and horizontal axes of each graph and the capacitor ratio K are given as per unit values. The actual values of the axis parameters can be

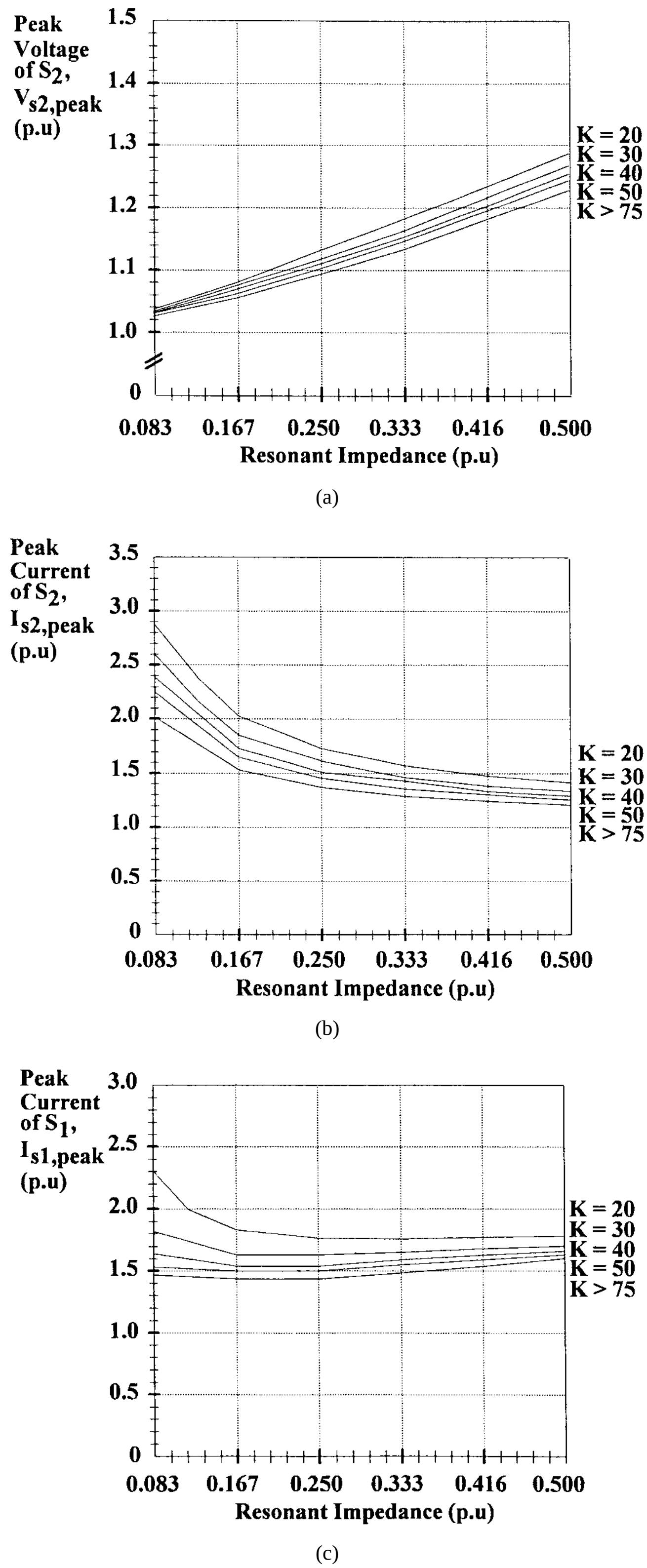

Fig. 4. (a) Peak voltage of S_2, $V_{s2,\text{peak}}$. (b) Peak current of S_2, $I_{s2,\text{peak}}$. (c) Peak current of S_1, $I_{s1,\text{peak}}$ versus resonant impedance Z_r for $Z_{rb} = 60\ \Omega$, auxiliary circuit transformer turns ratio $N_x = 8$, and various values of capacitor ratio K.

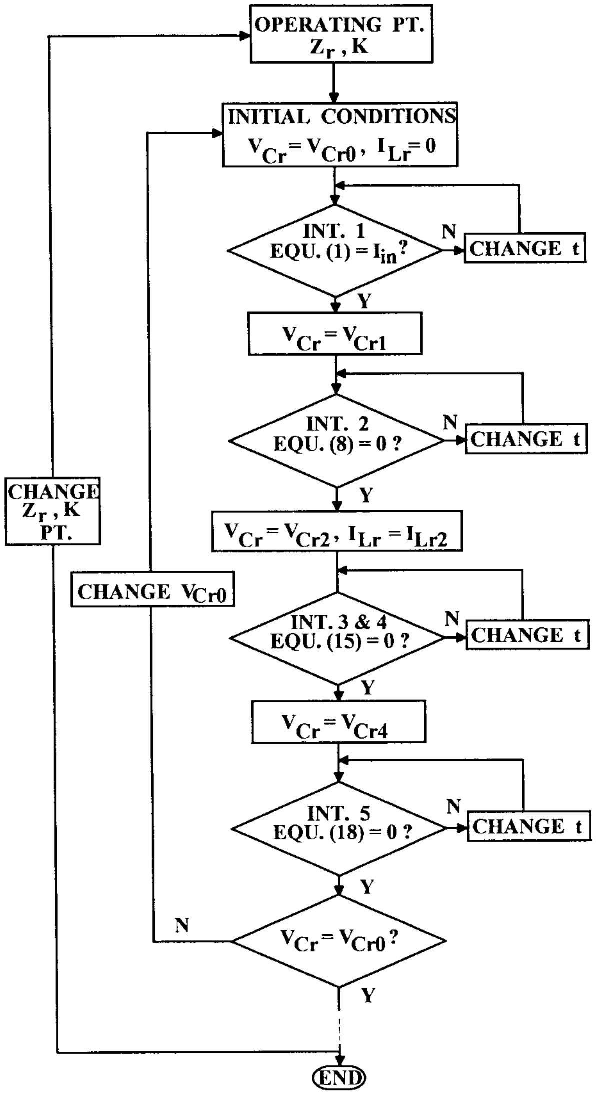

Fig. 5. Flowchart of program to determine if converter is operating under steady-state conditions.

obtained by multiplying the per unit value with the appropriate base value, as discussed in Section VI.

A. Auxiliary Switch Peak Voltage $V_{s2,\,\mathrm{peak}}$ Versus Auxiliary Circuit Resonant Impedance Z_r

A graph of auxiliary switch peak voltage $V_{s2,\,\mathrm{peak}}$ versus Z_r is shown in Fig. 4(a). The voltage across the switch when the auxiliary circuit is inactive is the sum of the output voltage V_o, the clamped transformer voltage V_x, and the voltage across Cr, V_{Cr}. It can be seen that $V_{s2,\,\mathrm{peak}}$ increases for increasing values of C_{s1} (decreasing values of K) if L_r and C_r (and therefore Z_r) are kept constant and increases for increasing values of L_r (increasing values of Z_r) if C_{s1} and C_r (and therefore K) are kept constant. In both cases, the reason is due to an increase in energy stored in C_r.

B. Auxiliary Switch Peak Current $I_{s2,\,\mathrm{peak}}$ Versus Auxiliary Circuit Resonant Impedance Z_r

A graph of auxiliary switch peak current $I_{s2,\,\mathrm{peak}}$ versus Z_r is shown in Fig. 4(b). It can be seen from this graph that if L_r and C_r (and therefore Z_r) are kept constant, then $I_{s2,\,\mathrm{peak}}$ increases for increasing values of C_{s1} (decreasing values of K) because there is more energy being discharged into the auxiliary circuit. If C_{s1} and C_r (and therefore K) are kept constant and L_r is varied instead, then $I_{s2,\,\mathrm{peak}}$ decreases for increasing values of L_r because this increases the value of Z_r, which is the characteristic impedance of the auxiliary resonant circuit.

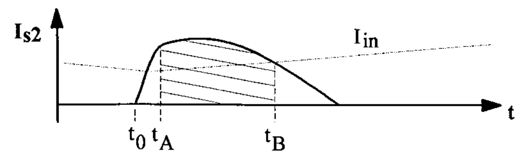

Fig. 6. Time interval during which S_1 should be turned on for ZVS turn on.

C. Main Switch Peak Current $I_{s1,\,\mathrm{peak}}$ Versus Auxiliary Circuit Resonant Impedance Z_r

The graph of main switch peak current $I_{s1,\,\mathrm{peak}}$ versus Z_r shown in Fig. 4(c) has the same characteristics as the graph in Fig. 4(b) until $Z_r > 15$–$20\ \Omega$ (0.250–0.333 p.u.) when the current rises. This can be explained by considering that the peak auxiliary circuit current during Interval 5 (when the main switch current becomes the sum of the auxiliary circuit and input currents) is proportional to V_{Cr4}/Z_r, where V_{Cr4} is the voltage across V_{Cr} after Interval 4 and is positive. Both V_{Cr4} and Z_r are increased when C_r is decreased, but V_{Cr4} increases more at higher values of Z_r, which in turn increases the ratio of V_{Cr4}/Z_r. The increase in V_{Cr4} when C_r is decreased also explains why the rise in $I_{s1,\,\mathrm{peak}}$ when $Z_r > 15$–20 becomes more pronounced at higher values of K.

V. Time Interval for ZVS Turn On of Main Switch S_1

The turns ratio N_x of transformer T_x determines the amount of energy circulating in the auxiliary circuit while it is operating. As N_x is lowered, less energy circulates in the circuit, which results in reduced auxiliary circuit voltages and currents. There is, however, a limit as to how low the value of N_x can be. If N_x is too low, then switch S_1 will not be able to turn on with ZVS.

The main switch will have a ZVS turn on only if it is turned on after capacitor C_{s1} has been discharged at time $t = t_A$, but before the current through the resonant circuit drops below the input current at $t = t_B$ (thus recharging C_{s1}) as shown in Fig. 6. This means that a ZVS turn on will occur as long as S_1 is turned on at a time instant within the time interval $t_A - t_B$ ($t = t_0^*$) after the auxiliary switch S_2 has been turned on at time t_0. When the auxiliary circuit is operating, the voltage across the primary of T_x is clamped to $V_x = V_o/N_x$. Since the polarity of V_x is set to be opposite that of V_{Cr}, the voltage across L_r and thus the current flowing in the auxiliary circuit I_{Lr} is reduced—the higher the value of V_x, the lower I_{Lr} is and therefore the lower the amount of energy available to discharge capacitor C_{s1}. Switch S_1 will not turn on with ZVS if V_x is set to too large a value.

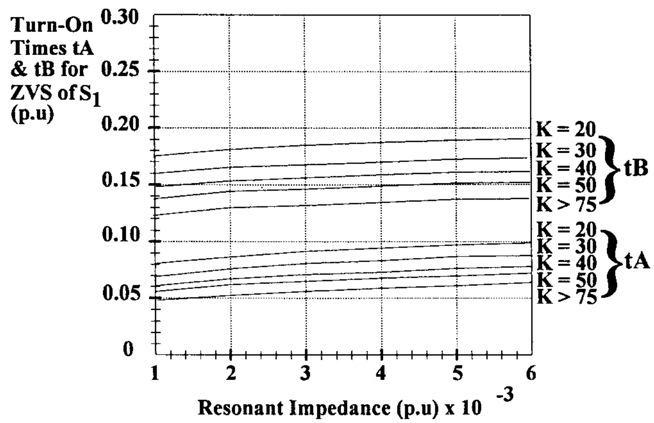

Fig. 7. ZVS turn-on times for S_1 per unitized with respect to T_r versus resonant impedance Z_r for $Z_{rb} = 500\ \Omega$, auxiliary circuit transformer turns ratio $N_x = 8$, and various values of capacitor ratio K.

The ZVS time interval $t_A - t_B$ is at its shortest when the input current is low. It is therefore at low values of input current that curves for t_A and t_B should be generated. For example, Fig. 7 shows curves of ZVS time interval $t_A - t_B$ generated with $Z_{rb} = Z_{rb,\max} = 500\ \Omega$ taken to be representative of the case when the input current is small. A ZVS turn on for S_1 will be guaranteed if $t = t_0^*$ is set so that it is between the t_A and t_B curves at this value of Z_{rb}. Note that t_A and t_B in Fig. 7 have been per unitized with respect to

$$T_r = 2\pi\sqrt{L_r C_r} \tag{22}$$

where T_r is the duration of the natural resonant cycle of the auxiliary circuit.

VI. Design Guidelines

In this section, guidelines for the design of the proposed converter are presented.

A. Selection of Boost Converter Components and Capacitor C_{s1}

The process of selecting boost converter components L_{in}, S_1, D_1, and C_o is the same as that for a conventional PWM boost converter. The design and rating of these components are the same except for the peak current of switch S_1, which occurs during a small fraction of the switching cycle. Since the peak current ratings of switches tend to be much higher than their continuous current ratings, the guidelines for selecting the switch are therefore the same as those used to select the switch in a conventional boost converter.

In a standard PWM boost converter, C_{s1} is the sum of the output capacitance of the main boost switch and an external capacitor placed across the switch. The purpose of the external capacitor is to further limit the losses and the EMI caused by the turn off of S_1—the larger the value of C_{s1}, the lower the losses and EMI are since C_{s1} slows down the rate of voltage rise across the switch. For the proposed converter, C_{s1} should be determined in the same manner as it is for a standard boost converter.

B. Selection of Transformer Turns Ratio and Diodes

The transformer turns ratio N_x should be selected so that it is high enough to allow S_1 to operate with soft switching, but low enough to keep voltage and current stresses low. N_x can be determined by generating time interval curves for the ZVS turn on of S_1, then determining whether a sufficient ZVS time interval exists for a wide range of resonant circuit component values. If such an interval does not exist, then curves should be generated for a higher value of N_x until a sufficient ZVS time interval arises.

The maximum voltage that a transformer secondary diode experiences is twice the output voltage when the other diode is conducting current. The peak and average current values of these diodes can be found by dividing the respective auxiliary current values by N_x. The average current flowing in the secondary diodes can be considered negligible since the auxiliary switch average current is already small.

C. Selection of Resonant Inductor L_r, Resonant Capacitor C_r, and Boost Diode

It was mentioned in the Introduction that one of the problems of the boost converter is the reverse recovery characteristic of the boost diode. This is partially a function of the diode's turn off di/dt and can be improved if the current flowing through it is slowly diverted during a controlled rise time after turning on S_2. This rise time is dependent on the value of inductor L_r. The larger the value of L_r, the less recovery current there will be, but there will also be more auxiliary circuit conduction losses as the length of the resonant cycle T_r, and thus the auxiliary circuit rms current, are increased. In order to minimize the amount of reverse recovery current while keeping L_r as small as possible, L_r can be designed so that the auxiliary circuit current is allowed to ramp up to within three times the boost diode's specified reverse recovery time, t_{rr}, as suggested in [5]. The value of L_r can be calculated for the proposed converter as follows:

$$L_r = \frac{3t_{rr}\left(V_{s2} - 2\dfrac{V_o}{N_x}\right)}{I_{\text{in,max}}}. \tag{23}$$

The value of $V_{s2} - 2V_o/N_x$ represents the voltage across L_r just after S_2 is turned on.

The value of C_r should be selected to be as low as possible to keep the length of the resonant cycle T_r small. If, however, the value of C_r is too low, then this will result in excessive values of $I_{s2,\text{peak}}$ and, more importantly, V_{s2}. As a compromise, the value of C_r should be selected so that it is small, but does not allow V_{s2} to exceed some specified limit. This tradeoff will be seen more clearly in the design example, where it is demonstrated how the value of C_r can be chosen by using design curves.

It should be noted that the boost diode D_1 should be a fast recovery diode because a slower diode would require a larger value of L_r, which would increase the duration of auxiliary circuit operation and conduction losses.

D. Selection of Auxiliary Switch S_2

The main criteria for the selection of auxiliary switch S_2 are the peak voltage and current values. The peak voltage and current ratings can be determined from characteristic curves such as the ones shown in Fig. 4. Once these ratings have been determined, a device for the auxiliary switch can be chosen from among several devices. The output capacitance of the device C_{s2} should be as low as possible in order to minimize the losses that still exist when the switch is turned on with ZCS. The on-state resistance of the device R_r should also be low in order to reduce conduction losses. Since output capacitance and on-state resistance are inversely related in MOSFET's (a decrease in one means an increase in the other), a compromise must be made between the two in choosing a device. For example, a MOSFET with an on-state resistance in the low milliohms would not be recommended because its high value of output capacitance would result in high switching losses. To help in the selection of S_2, the following equation can be used to approximate the losses in the device:

$$S_{2,\text{loss}} = \frac{C_{s2} V_{s2} f_{\text{sw}}}{2} + 0.2(I_{s2,\,\text{peak}}^2 T_r f_{\text{sw}}) R_r. \tag{24}$$

It has been assumed for (24) that the current flowing through S_2 is like a clipped half-wave sinusoid and that auxiliary circuit operation is insensitive to variations in R_r.

VII. Design Procedure and Example

A design procedure to select the auxiliary circuit components and the ZVS time interval $t_A - t_B$ for the S_1 turn on are presented in this section. The procedure is based on the guidelines that were presented in the previous section. The key design objective is to select values for L_r and C_r so that the following is achieved.

1) The boost diode reverse recovery current is eliminated.
2) The voltage across S_2 is kept below a targeted value (i.e., the maximum allowable switch voltage).
3) Switch S_1 turns on with ZVS (capacitor C_{s1} ensures that S_1 turns off with ZVS).

The steps of the design procedure are as follows.

1) Select components L_{in}, S_1, D_1, C_o, and C_{s1} using the same procedure as that used to design a conventional PWM boost converter.
2) Generate curves of t_A and t_B versus Z_r for various values of N_x and $K = C_r/C_{s1}$. Select a value of N_x that allows for the ZVS turn on of S_1 over a wide range of values of Z_r (i.e., 5–20 Ω). This should be done for a high value of Z_{rb} (i.e., $Z_{rb,\max} > 200$) because the ZVS time interval is the shortest when the input current is low. Note that it is pointless to design for $Z_{rb,\max} = \infty$, which corresponds to zero-input current because the main switch has no switching losses in this case.
3) Determine the lowest value of $Z_{rb} = V_o/I_{\text{in}}$, $Z_{rb,\min}$ that the converter can encounter just before the auxiliary circuit is activated, and take this value to be the base impedance. This is when the main switch and auxiliary switch peak currents and the auxiliary switch voltage are at their highest values. The base voltage is V_o, and the base current is the corresponding input current.
4) Use (23) to determine a value for L_r that will eliminate the boost diode reverse recovery current.
5) Use a graph of auxiliary switch voltage such as the one in Fig. 4(a) to determine the smallest value of C_r that makes $V_{s2,\,\text{peak}}$ to be less than the targeted value.
6) When N_x, L_r, and C_r (and thus Z_r) are known, determine the ratings for the auxiliary switch and the ZVS time interval.

TABLE I
Base Values

VOLTAGE	$V_b = 380$ V
CURRENT	$I_b = 6.3$ A
IMPEDANCE	$Z_{rb,\min} = 60\,\Omega$ (Fig. 4)
	$Z_{rb,\max} = 500\,\Omega$ (Fig. 7)
TIME	$T_b = 2.76\,\mu$s

The following example is given to illustrate the design procedure. It should be noted that the design procedure is an iterative one, and that only the last iteration is shown. The converter is to be designed according to these specifications.

Output power	$P_0 = 500$ W.
Output voltage	$V_o = 380$ V.
Input voltage	$V_{\text{in}} = 100 - 240$ Vrms.
Switching frequency	$f_{\text{sw}} = 50$ kHz.
Maximum voltage of S_2	$V_{s2,\,\text{peak}} \leq 1.2V_o$.
Input current peak ripple	$I_{\text{in,rip}} = 15\%$.
Output voltage peak ripple	$V_{\text{cor,pk}} = 1\%$.

The voltage across the auxiliary switch V_{s2} is targeted to be less than or equal to $1.2V_o$ so that a 500-V device can be used as the auxiliary switch. This gives a safety margin of about 50 V for the worst case condition. For the design example, it will be assumed that the converter efficiency is $\eta = 95\%$ at low-input voltage and that $V_{\text{cor,pk}}$ is negligible. The base values used for per unitizing are listed in Table I. The steps taken in the example are as follows.

1) The procedure to select components L_{in}, S_1, D_1, and C_o is shown in [10] and will therefore not be shown here. C_{s1} is set to 0.75 nF, and the boost diode to be used is a fast recovery diode with a reverse recovery time of $t_{rr} = 60$ ns.
2) A transformer turns ratio of $N_x = 8$ is selected based on the graph shown in Fig. 7. It can be seen that a ZVS time interval $t_A - t_B$ exists over a wide range of Z_r when the input current is low (i.e., $Z_{rb,\max} = 500$). This is the worst case condition for operating S_1 with a ZVS turn on. Lower values of N_x such as $N_x = 6$ or 7 were rejected because they did not provide a sufficient ZVS time interval for the main switch.
3) The minimum value of $Z_{rb,\min} = V_o/I_{\text{in}}$ that the converter will encounter just before the auxiliary circuit is activated is when the input current is at its peak, when $V_{\text{in}} = 100$ Vrms. This current value can be calculated

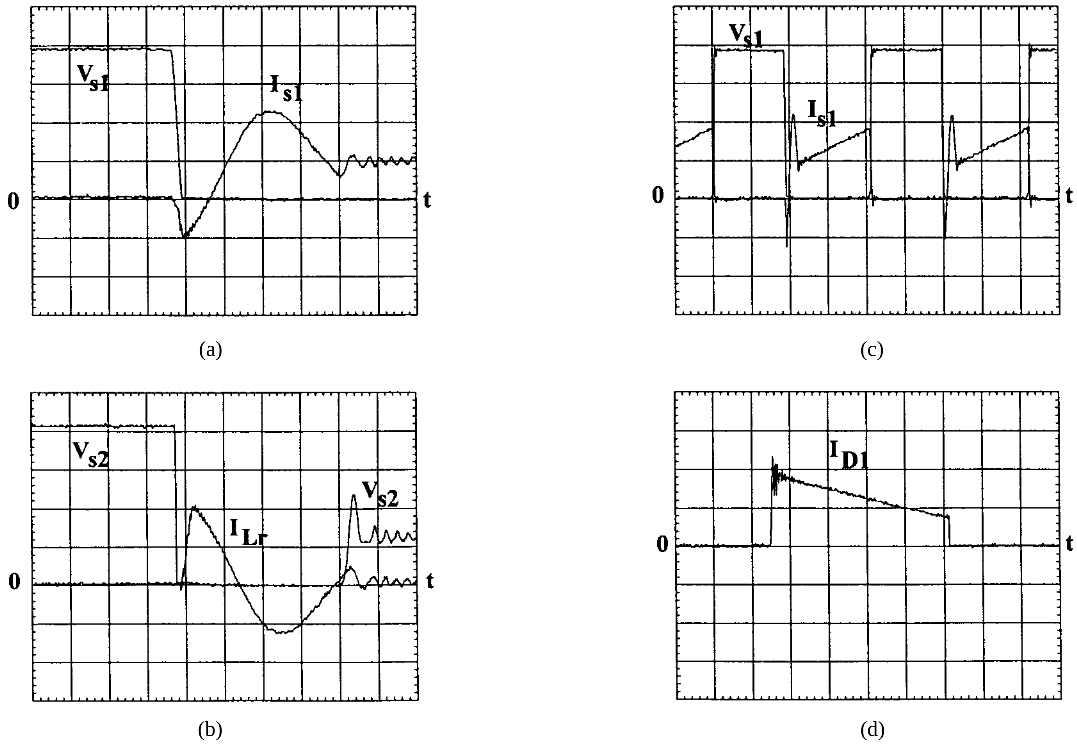

Fig. 8. Experimental results: $V_o = 380$ V and $P_o = 500$ W. (a) Main switch S_1 turn on (V: 100 V/div, I: 2 A/div, and t: 500 ns/div). (b) Auxiliary switch S_2 voltage and resonant inductor current (V: 100 V/div, I: 2 A/div, and t: 500 ns/div). (c) Main switch S_1 waveforms (V: 100 V/div, I: 2 A/div, and t: 5 s/div). (d) Boost diode current (I: 2 A/div and t: 2 s/div).

as follows:

$$I_{\text{in}} = \frac{\sqrt{2}\cdot P_o}{V_{\text{in}}\eta}\,(1-\Delta I_{\text{in,rip}}) = \frac{\sqrt{2}\cdot 500}{100\cdot 0.95}\,(1-0.15) = 6.3\text{ A}. \tag{25}$$

Note that the input peak current ripple of 15% has been taken into account because the current is below its average value when auxiliary circuit is activated and it starts to rise afterwards while S_1 is on. The minimum value of Z_{rb} is $Z_{rb,\min} = 380/6.3 = 60\ \Omega$. The curves in Fig. 4 which have already been generated for $Z_{rb} = 60\ \Omega$ will be used in this example.

4) The value of L_r is determined from (23)

$$L_r = \frac{3(60\text{ ns})\,(1.2\cdot 380\text{ V} - 2\frac{380}{8})}{6.3\text{ A}} = 10.3\,\mu\text{H}. \tag{26}$$

5) The smallest value of C_r so that $V_{s2,\text{peak}} \le 1.2$ p.u. can be found from Fig. 4(a). This can be approximated to be $C_r = 0.75\text{ nF}\times 25 = 18.8$ nF at $Z_r = 22\ \Omega$ (0.367 p.u.) and $K = 25$. $V_{s2,\text{peak}} = 1.2\text{ V}\times 380$ p.u. $= 456$ V. Note that a larger value of C_r could have been chosen to make $V_{s2,\text{peak}}$ to be less than 1.2 p.u., but this would have meant increasing the duration of the auxiliary circuit resonant cycle.

6) $I_{s2,\text{peak}}$ and $I_{s1,\text{peak}}$ are found from Fig. 4(b) and (c). For $K = 25$ and $Z_r = 22\ \Omega$, $I_{s2,\text{peak}} \approx 6.3\text{ A}\times 1.45$ p.u. $= 9.2$ A and $I_{s1,\text{peak}} \approx 6.3\text{ A}\times 1.7$ p.u. $= 10.8$ A. For the ZVS time interval graph of Fig. 7, the value of T_r is calculated using (22)

$$T_r = 2\pi\sqrt{10.3\,\mu\text{H}\cdot 18.8\,\text{nF}} = 2.76\,\mu\text{s}. \tag{27}$$

The values of t_A and t_B from Fig. 7 for $K = 25$ and $Z_r = 22$: $t_A = 0.085\times 2.76$ s $= 235$ ns and $t_B = 0.17\times 2.76$ s $= 470$ ns. The peak voltage stress across the transformer diodes is 2 p.u. or $2\times 380\text{ V} = 760$ V.

VIII. Experimental Results

The feasibility of the proposed converter was verified with results obtained from a 500-W experimental prototype. The input voltage was 100–240 Vrms, the output voltage was $V_o = 380$ V, and the switching frequency was 50 kHz. The auxiliary circuit component values that were used were $L_r = 9.8\ \mu$H and $C_r = 18$ nF. The main circuit component values were $C_{s1} = 0.75$ nF, $L_{\text{in}} = 800\ \mu$H, and $C_o = 780\ \mu$F. An IRFP460 MOSFET was used as the main switch, an IRF840 MOSFET was used as the auxiliary switch, and a HFA15TB60 fast recovery diode was used as the boost diode. A Micrometals T106-8/90 core was used for L_r, and a TDK PC30 core was used for the transformer.

Fig. 8(a) shows the voltage across the main switch S_1 and the combined current through S_1, its body diode, and capacitor C_{s1}. It can be seen that C_{s1} is discharged and there are no switching losses during turn on. Fig. 8(b) shows auxiliary switch voltage and resonant inductor current waveforms. It can be seen that the switch has a ZCS turn on and that current does flow through the antiparallel diode across the auxiliary

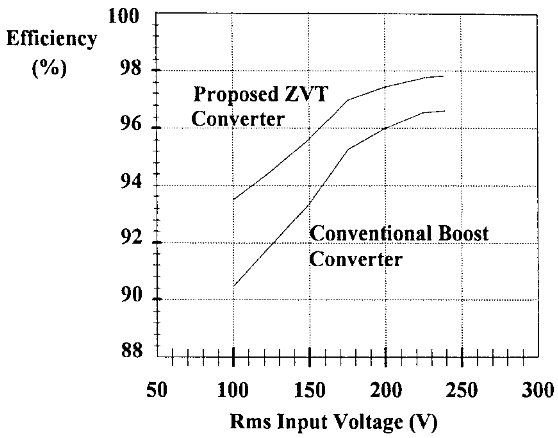

Fig. 9. Efficiency versus rms input voltage ($V_o = 380$ V, $P_o = 500$ W, and $f_{\mathrm{sw}} = 50$ kHz).

switch thus ensuring that the switch has a ZVS turn off with very little ringing.

Fig. 8(c) shows the same pair of waveforms as in Fig. 8(a), but on a different time scale. These waveforms are the same as those found on a PWM boost converter although the current does have a resonant peak due to the auxiliary circuit. Fig. 8(d) shows the current flowing through the boost diode. Note that there is no reverse recovery current—this is due to the operation of the auxiliary circuit. Fig. 9 shows the efficiency of the proposed converter as a function of input voltage compared with that of a conventional PWM converter. It can be seen that the proposed converter is more efficient than the PWM converter, especially when the input voltage is low.

IX. Conclusion

A ZVT PWM boost converter has been proposed in this paper. The key feature of this converter is that a nearly lossless auxiliary switch turn off is achieved with a soft instead of a hard turn off, which limits EMI. Additional features include PWM control with soft switching for all active and passive switches, and low peak switch stresses due to a simple energy feedforward auxiliary circuit. The operation of the converter has been explained and analyzed. The results of the analysis have been used to generate characteristic curves that were then used to develop guidelines for the design of converter components and for ZVS operation. The results obtained from a 500-W prototype have shown that the proposed converter can operate with little increase in voltage and current stresses and that an improvement in efficiency of approximately 2%–3% over the conventional PWM converter can be achieved.

References

[1] R. Streit and D. Tollik, "High efficiency telecom rectifier using a novel soft-switching boost-based input current shaper," in *IEEE Int. Telecom. Ener. Conf. Rec.*, 1991, pp. 720–726.

[2] G. Hua, C.-S. Lieu, Y. Jiang, and F. C. Lee, "Novel zero-voltage-transition PWM converters," *IEEE Trans. Power Electron.*, vol. 9, pp. 213–219, Mar. 1994.

[3] L. Yang and C. Q. Lee, "Analysis and design of boost zero-voltage-transition PWM converter," in *IEEE Appl. Power Elec. Conf. Rec.*, 1993, pp. 707–713.

[4] J. P. Gegner and C. Q. Lee, "Zero-voltage-transition converters using a simple magnetic feedback technique," in *IEEE Appl. Power Elec. Conf. Rec.*, 1994, pp. 590–596.

[5] J. Bazinet and J. O'Connor, "Analysis and design of a zero-voltage-transition power factor correction circuit," in *IEEE Appl. Power Elec. Conf. Rec.*, 1994, pp. 591–600.

[6] G. Moschopoulos, P. Jain, and G. Joos, "A novel zero-voltage switched PWM boost converter," in *IEEE Power Elec. Spec. Conf. Rec.*, 1995, pp. 694–700.

[7] K. M. Smith and K. M. Smedley, "A comparison of voltage mode soft switching methods for PWM converters," *IEEE Trans. Power Electron.*, vol. 12, pp. 376–386, Mar. 1994.

[8] D. Zhang, D. Y. Chen, and F. C. Lee, "An experimental comparison of conducted EMI emission between a zero-voltage transition circuit and a hard switching circuit," in *IEEE Power Elec. Spec. Conf. Rec.*, 1996, pp. 1992–1997.

[9] G. Moschopoulos, "Soft-switching power factor corrected converter topologies," Ph.D. dissertation, Concordia Univ., Montréal, P.Q., Canada, 1996.

[10] L. H. Dixon, "High power factor switching preregulator design optimization," in *Unitrode Power Supply Design Seminar SEM700*, 1990.

Gerry Moschopoulos (S'90–M'97) received the B.Sc., M.A.Sc., and Ph.D. degrees in electrical engineering from Concordia University, Montréal, P.Q., Canada, in 1989, 1992, and 1997, respectively.

From 1995 to 1998, he was with the Advanced Power Systems Division, Nortel, where he worked on the development of power supplies and systems for telecommunications applications. He is now with the Department of Electrical and Computer Engineering, Concordia University, where he researches the application of power electronics for telecommunications and computer systems.

Praveen K. Jain (S'86–M'88–SM'91) received the B.E. (Hons.) degree from the University of Allahabad, India, and the M.A.Sc. and Ph.D. degrees from the University of Toronto, Toronto, Ont., Canada, in 1980, 1984, and 1987, respectively, all in electrical engineering.

Currently, he is a Professor at Concordia University, Montréal, P.Q., Canada, where he is engaged in teaching and research in the field of power electronics. Prior to this (1989–1994), he was a Technical Advisor with the Power Group, Nortel, Ottawa, Ont., where he provided guidance for research and development of advanced power technologies for telecommunications. During 1987–1989, he was with Canadian Astronautics Ltd., Ottawa, where he played a key role in the design and development of high-frequency power conversion equipment for the Space Station Freedom. He was a Design Engineer and Production Engineering at Brown Boveri Company and Crompton Greaves Ltd., India, respectively, from 1980 to 1981. He has published over 100 technical papers and holds nine patents (an additional ten are pending) in the area of power electronics. His current research interests are power electronics applications to space, telecommunications, and computer systems.

Dr. Jain is a member of the Professional Engineers of Ontario and an Associate Editor of the IEEE Transactions on Power Electronics.

Yan-Fei Liu (S'90–M'94–SM'97) received the B.Sc. and M.Sc. degrees from Zhejiang University, Hangzhou, China, in 1984 and 1987, respectively, and the Ph.D. degree from Queen's University, Kingston, Ont., Canada, in 1994.

He was an Assistant Professor at Zhejiang University from 1987 to 1990. In February 1994, he was a Design Engineer at the Advanced Power Systems Division of Nortel. Since September 1998, he has been a Design Engineer with the Advanced Power Systems Division, Astec, Ottawa, Ont. His research interests include new circuit configurations of low-switching loss dc-to-dc and ac-to-ac converters, low-output voltage power converters, computer simulation of switching power supplies, control techniques to improve dynamic performance of PWM switching converters, and dynamic modeling of PWM converters.

Géza Joós (M'79–SM'89) received the M.Eng. and Ph.D. degrees from McGill University, Montréal, P.Q., Canada, in 1974 and 1987, respectively.

Since 1988, he has been with the Department of Electrical and Computer Engineering, Concordia University, Montréal, where he is engaged in teaching and research in the areas of power converters and electrical drives. From 1975 to 1978, he was a Design Engineer with Brown Boveri Canada, and from 1978 to 1988, he was a Professor at the Ecole de Technologie Supérieure, Montréal.